Simulation of Viscous Textile Composite Sheet Forming Based on a Unit Cell Energy Model

P. Harrison[1], W.R. Yu[2], A. C. Long[1] and M.J. Clifford[1]

[1] *School of Mechanical, Materials and Manufacturing Engineering, The University of Nottingham, University Park, Nottingham NG7 2RD, U.K.*
[2]*School of Materials Science and Engineering, Seoul National University, Seoul, South Korea*
e-mail: philip.harrison@nottingham.ac.uk

ABSTRACT
An explicit commercial Finite Element (FE) code is used to simulate the forming of a thermoplastic viscous textile composite sheet over a hemispherical tool. The main success of this work is in combining two distinct models. The first model is a non-orthogonal rate-independent constitutive model that has been implemented previously in a commercial FE code [1, 2]. The second is a rate and temperature dependent unit cell energy model [3, 4], designed to predict the shear force – shear angle – shear rate response of viscous textile composites. The combined implementation of these two models in the explicit FE code means that, given the fibre volume fraction and matrix rheology of the composite sheet, accurate predictions of the material's forming behaviour can be performed without the need for extensive material characterisation experiments. Both models are reviewed briefly and the method of combining these models in the code is described. Finally, results of preliminary forming simulations using a hemispherical tool are presented and discussed.

1. INTRODUCTION
Virtual technology is an important tool in improving efficiency in automated manufacturing processes. As such, deep drawing and press forming of viscous textile composites, including thermosetting prepregs and fabric reinforced thermoplastics, are prime candidates for virtual process development. Competition between composites and metals has created strong demand for such simulation technology in the composites industry, resulting in considerable research interest in the field. In the past, two main approaches have been followed in the forming simulation of viscous textile composites, namely the development of algorithms based on pin-jointed net kinematics and the Finite Element (FE) method. In this investigation we concentrate on the FE method.

A non-orthogonal constitutive model implemented previously in a commercial FE code (Abaqus Standard™ and Explicit™) is used to incorporate predictions from a constituent based unit cell energy model [1, 2]. As it stands this non-orthogonal model is rate-independent. However, by linking the shear parameters of the non-orthogonal model to predictions of the energy model [3, 4], both rate and temperature effects can be included in the simulations. The main role of the energy model is to predict the shear force – shear angle – shear rate behaviour of viscous textile composites using material parameters supplied readily by material manufacturers, such as fibre volume fraction, weave architecture and matrix rheology. The motives for such constituent-based predictive modelling are two-fold. First, once the material behaviours of the constituent components are known then the rheology of any composite comprised of matrix and continuous inextensible fibres can be predicted, allowing the pre-manufacturing optimisation of a composite to suit a potential application. Second, characterising the rheological behaviour of, for example, a thermoplastic matrix polymer at different shear rates and temperatures is relatively easy using modern rheometers, compared with the equivalent but more difficult task of characterising the rheology of textile composites using picture frame and bias extension tests [5]. Success in both these issues would lead to significant reductions in time and cost in the manufacturing process. The structure of this paper is as follows. The energy model is summarised followed by a brief description of the non-orthogonal model. Full descriptions of these models can be found elsewhere [1-4]. The method of incorporating

predictions of the energy model in the non-orthogonal model is outlined. Rate dependent FE predictions are made using the combined models and comparisons are drawn with rate-independent FE predictions. The results are discussed and potential further improvements are suggested.

2. MICRO-MECHANICAL MODEL

During shear, it has been observed that the in-plane shear strain rate of tows is rarely as high as the overall in-plane shear rate across the composite sheet [3]. This produces a discontinuous shear strain profile across the sheet with most of the shear strain concentrated in inter-tow regions. An example of such a non-linear shear profile is shown in Fig 1.

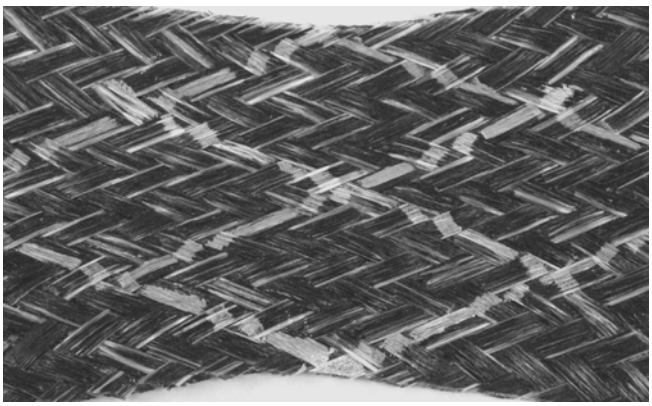

Fig 1. Example of discontinuous shear strain profiles across a textile composite. The broken form of initially continuous lines drawn on the fabric before shear, serves to illustrate the strain profiles. 2 x 2 twill weave glass/polypropylene thermoplastic sheared in a bias extension test at 180^{o}C.

These observed kinematics have motivated the use of a novel two-phase material model structure to analyse the energy dissipation within the textile composite. For the purpose of the model, the textile is considered to consist of two distinct superposed layers, each consisting of parallel tows and inter-tow regions, see Fig 2. Each tow is modelled as a volume of uniaxial Ideal Fibre Reinforce Fluid (IFRF) whereas the inter-tow regions are filled with isotropic matrix fluid. The observed kinematics have important consequences for the deformation occurring during shear of textile composites, both within tow (fibre bundle) and inter-tow regions, and also between tow crossovers.

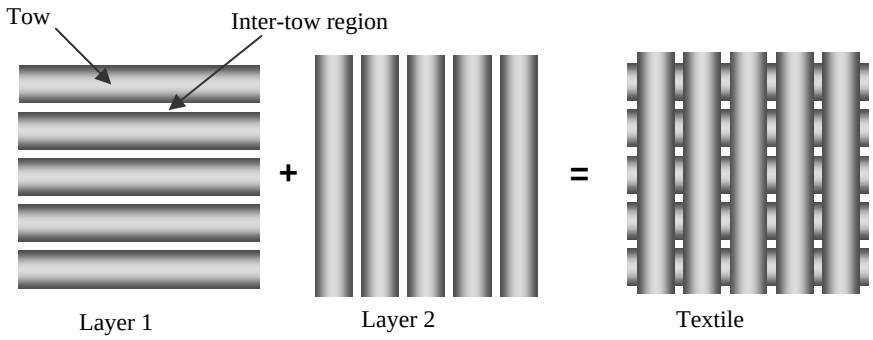

Fig. 2. Textile modelled as two superposed layers of uniaxial composite consisting of tow and inter-tow regions.

Considering, for example, the rate of deformation tensor, the discontinuous shear profile means that $2D_{ij}$ must be re-derived for both the tow and inter-tow regions. In order to do this it is necessary to define a set of coordinate systems, see Fig. 3.

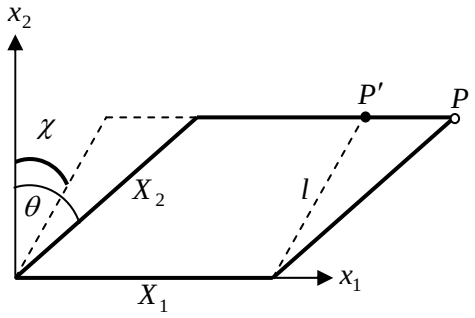

Fig 3. Coordinate system. θ is the material shear angle, χ is the shear angle of this local region (indicated by dashed lines).

The first coordinate system, x_i, describes a fixed Cartesian system. A second material coordinate system, X_i, is considered attached to and to deform with each point, *P*, of a continuum in a hypothetical material undergoing homogeneous deformation. This is referred to here as the material coordinate system. Note that for the case of heterogeneous shear, particles of the localised continuum attached to the tows or inter-tow regions, referred to here by *P'*, are no longer stationary in the material coordinate system. Fig. 3 shows the deformation imposed in the tow regions. In the case shown, χ corresponds to the tow shear angle, χ_t, where $0 \le \chi_t \le \theta$ and where θ is the material shear angle. The derivation also applies to the inter-tow region, however, in that case, χ would correspond to the shear angle of the inter-tow region, χ_m. The fibre direction is considered parallel to the X_1 axis of the fixed frame. It can be shown that in this reference frame,

$$2D_{ij} = \begin{bmatrix} 0 & \left(\dot{\chi}\sec^2\chi - \dot{\theta}\tan\theta\tan\chi\right) & 0 \\ \left(\dot{\chi}\sec^2\chi - \dot{\theta}\tan\theta\tan\chi\right) & -2\dot{\theta}\tan\theta & 0 \\ 0 & 0 & 2\dot{\theta}\tan\theta \end{bmatrix} \tag{1}$$

where $\dot{\theta}$ is the relative angular velocity of the two reinforcement directions in the textile. From Eq. (1) the simple shear rate of the tows or inter-tow regions, $\dot{\gamma}_t$ or $\dot{\gamma}_m$, is given as

$$\dot{\gamma} = \dot{\chi}\sec^2\chi - \dot{\theta}\tan\theta\tan\chi \tag{2}$$

where χ and $\dot{\chi}$ must be chosen accordingly to represent either the tow or inter-tow shear angle. From Eq. (2) is can be shown that when $\dot{\chi} = \dot{\theta}$ at all times (the condition of homogeneous shear) then $\dot{\gamma} = \dot{\theta}$. Using tensor notation, the constitutive equation for a uniaxial IFRF [6], is given by Eq. (3)

$$\sigma_{ij} = -p\delta_{ij} + T_a a_i a_j + 2\eta_T D_{ij} + 2(\eta_L - \eta_T)\left(a_i a_k D_{kj} + a_j a_k D_{ki}\right) \tag{3}$$

where δ_{ij} denotes the unit tensor, a_i defines the direction of the fibre reinforcement, $-p\delta_{ij}$ and $T_a a_i a_j$ are reaction stresses due to the constraints of incompressibility and fibre inextensibility, η_T and η_L are the transverse and longitudinal viscosity parameters and *i*, *j* and *k* range from 1 to 3. Using micro-mechanical modelling principals [7, 8] both η_T and η_L can be predicted from the matrix viscosity, η_m, and fibre volume fraction. The interaction between fibres and matrix occurs on a microscopic scale and is shown in the schematic of Fig. 4. Here the transverse viscosity, η_T, results from individual fibres rolling past one another, while the longitudinal viscosity, η_L, results from the fibres sliding past one another along their length. Numerous ingenious experiments have been devised to measure these two viscosities [e.g. 9-11]. It should be noted that viscosity parameters appearing in the constitutive equations of biaxial IFRF [12, 13] can not be related to micro-mechanical mechanisms, precluding the possibility of developing constituent based models based on biaxial IFRF model theory.

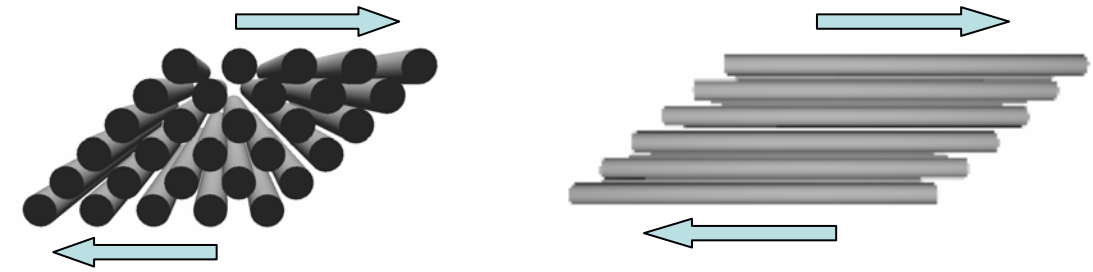

Fig 4. (a) Shearing the composite across or transverse to the fibre direction gives a measure of the transverse viscosity and (b) shearing the composite parallel to the fibre direction gives a measure of the longitudinal viscosity.

Using Eq. (1) and (3) together with the plane stress condition, it is possible to determine the rate of energy dissipation of the combined tow and inter-tow regions during shear using an expression for the stress power, dE/dt, of the deforming material [14],

$$\frac{dE}{dt} = W_o T\left(4\eta_T \dot{\theta}^2 \tan^2\theta + \eta_L \dot{\gamma}_t^2\right) + w_o T q \eta_m \left(4\dot{\theta}\tan^2\theta + \dot{\gamma}_m^2\right) \tag{4}$$

where W_o and w_o are the initial widths of the tow and inter-tow regions, T is the thickness of the sheet, q is a factor related to the fabric architecture and $\dot{\gamma}_t$ and $\dot{\gamma}_m$ are found using Eq. (2). However, while the analysis described above accounts for the energy dissipation within the tow and inter-tow regions, the heterogeneous strain profile also induces energy dissipation between the tow crossovers. The velocity field between crossovers is calculated by analysing the in-plane kinematics of tow deformation during shear [3, 4]. The resulting velocity field between crossovers is

$$\vec{v}_{rel} = \left\{\left(\dot{\gamma}_t - \dot{\theta}\right)\left(1-\sin\theta\right)Y\right\}\hat{\mathbf{i}} + \left\{\left(\dot{\theta} - \dot{\gamma}_t\right)\left(1-\sin\theta\right)X\right\}\hat{\mathbf{j}} \tag{5}$$

where the unit vectors, $\hat{\mathbf{i}}$ and $\hat{\mathbf{j}}$ are orthogonal and coincide with the fibre reinforcement bisector directions and X and Y are the position coordinates in this reference frame. By measuring the tow shear kinematics and using Eq. (3) it is possible to calculate the velocity field between the tow crossovers (future refinements of the model will allow prediction of the tow shear kinematics). The thickness of the matrix film separating tows at the tow crossovers can be estimated from the fibre

volume fraction. Using the velocity field and matrix film thickness the shear strain rate in the matrix film can be estimated as a function of position. Finally, given the matrix viscosity, an estimate of the rate of energy dissipation can be determined due to shear between tow crossovers. By combining the energy contributions from both tow/inter-tow shear and crossover shear, the total rate of energy dissipation during shear of the textile composite can be estimated and from this the shear force can be determined.

3. NON-ORTHOGONAL MODEL

To model the stress and strain relationship dependent on the fibre directional properties, a non-orthogonal equation has been developed in an explicit mathematical form by using a homogenization method [1]. The resulting 2-D equation is based on a structural net concept (see Fig. 5) and its derivation follows two distinct steps [1].

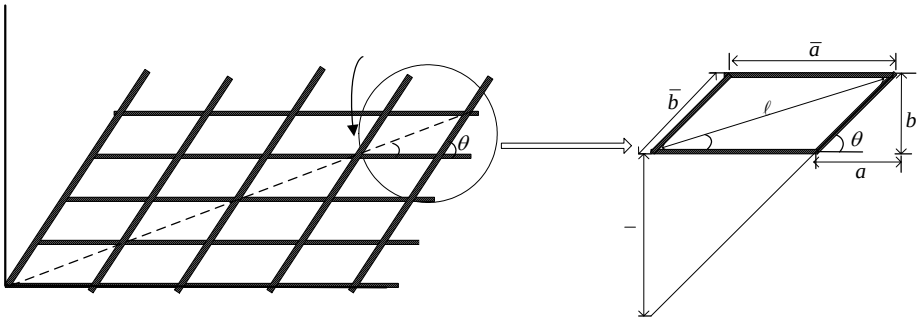

Fig 5. A structural net (left) and unit cell (right) of fabric reinforcement.

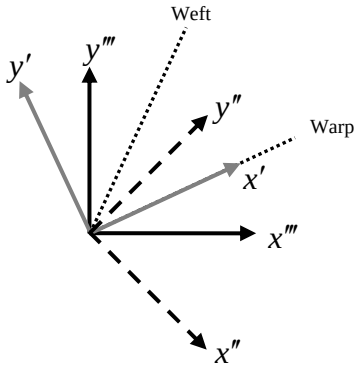

Fig 6. Warp and weft fibre reinforcement directions plus three orthogonal reference frames used in analysis. Single dashed system has *x*-axis collinear with warp reinforcement direction (reference frame of Eq. (6)). Double dashed system bisects the two fibre directions (reference frame of Eq (7)). Triple dashed system is material reference frame used in FE analysis (Eq. (6) and (7) are transformed to this system before addition).

Firstly, the contribution to total stress due to tensile strain in the non-orthogonal fibres is derived in a materially embedded orthogonal reference frame, with its *x*-axis co-linear with the fabric warp reinforcement direction (single dash system in Fig 6). The resulting tensile equation, Eq (6), relates incremental stress to incremental strain in this reference system. In this first step of the derivation the warp and weft fibres are assumed to rotate freely at crossover contact points assuming no frictional resistance.

y

$$\begin{bmatrix}\Delta\sigma_{xx}\\ \Delta\sigma_{yy}\\ \Delta\sigma_{xy}\end{bmatrix}=\begin{bmatrix}\dfrac{\tilde{E}^{\alpha}}{bc}+\Gamma\left(\dfrac{a}{\bar{\bar{h}}}\right)\left(\dfrac{a^2}{c}\right) & \Gamma\left(\dfrac{a}{\bar{\bar{h}}}\right)\left(\dfrac{b^2}{c}\right) & \Gamma\left(\dfrac{a}{\bar{\bar{h}}}\right)\left(\dfrac{ab}{c}\right)\\ \Gamma\left(\dfrac{b}{\bar{a}}\right)\left(\dfrac{a^2}{c}\right) & \Gamma\left(\dfrac{b}{\bar{a}}\right)\left(\dfrac{b^2}{c}\right) & \Gamma\left(\dfrac{b}{\bar{a}}\right)\left(\dfrac{ab}{c}\right)\\ \Gamma\left(\dfrac{b}{\bar{\bar{h}}}\right)\left(\dfrac{a^2}{c}\right) & \Gamma\left(\dfrac{b}{\bar{\bar{h}}}\right)\left(\dfrac{b^2}{c}\right) & \Gamma\left(\dfrac{b}{\bar{\bar{h}}}\right)\left(\dfrac{ab}{c}\right)\end{bmatrix}\begin{bmatrix}\Delta\varepsilon_{xx}\\ \Delta\varepsilon_{yy}\\ 2\Delta\varepsilon_{xy}\end{bmatrix} \tag{6}$$

where $\Delta\sigma$ and $\Delta\varepsilon$ are the stress and strain increments, *a*, *b* and *c* are related to the fabric geometry (see Fig. 5) and $\tilde{E}^{\alpha}$ and Γ are representative of the tensile stiffness of the warp and weft yarns [1]. In a second step, shear force versus shear angle data is related to the shear stiffness using a non-orthogonal covariant reference frame. The incremental stress due to shear is then transformed into the orthogonal fibre bisector frame (double dash system shown in Fig. 6) and related to the fibre shear angle increment, $\Delta\gamma$, as

$$\Delta\boldsymbol{\sigma}=\begin{bmatrix}\Delta\sigma_{xx}\\ \Delta\sigma_{yy}\\ \Delta\sigma_{xy}\end{bmatrix}=\begin{bmatrix}0 & 0 & 2G_1g_1^1g_2^1+G_2\left(g_1^1g_2^2-g_1^2g_2^1\right)\\ 0 & 0 & 2G_1g_1^2g_2^2+G_2\left(g_1^1g_2^2-g_1^2g_2^1\right)\\ 0 & 0 & G_1\left(g_1^1g_2^2+g_2^1g_1^2\right)\end{bmatrix}\begin{bmatrix}0\\ 0\\ \Delta\gamma\end{bmatrix} \tag{7}$$

where G_1 and G_2 are model parameters that can be related explicitly to the shear force versus shear angle curve, g_1^1, g_1^2 are components, expressed in the orthogonal fibre bisector frame (see Fig. 6), of $\hat{\mathbf{g}}_1$, a unit covariant base vector that convects with the warp fibre direction (see Fig. 7). Similarly, g_2^1, g_2^2 are components of $\hat{\mathbf{g}}_2$, a unit covariant base vector that convects with the weft fibre direction [2].

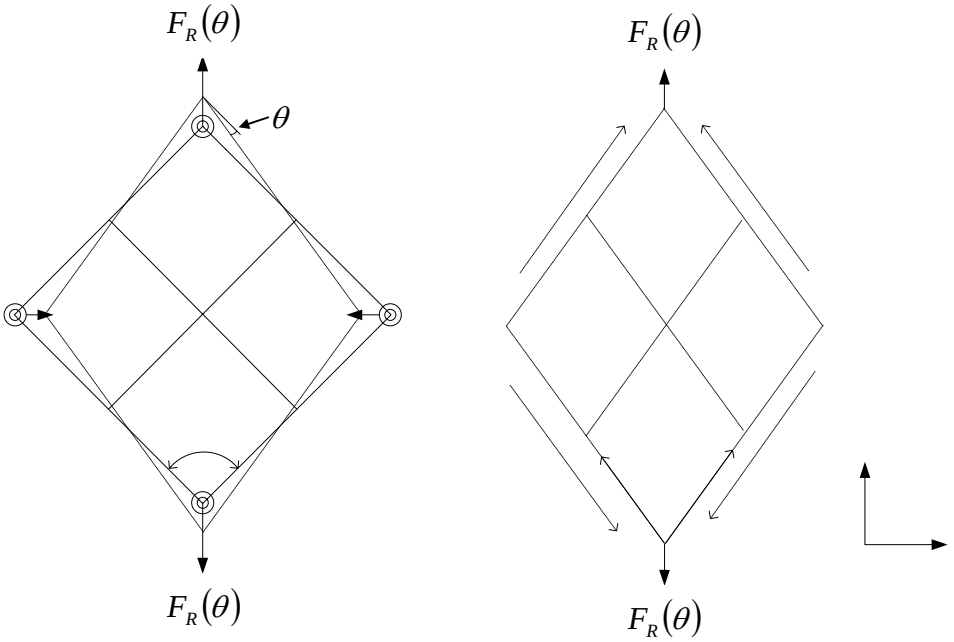

Fig 7. Schematics of the picture-frame shear test (left) and contra-variant stress (σ^{12}, σ^{21}) components acting along normalized covariant based vectors ($\mathbf{g}_1, \mathbf{g}_2$). The unit vectors $\mathbf{E_1}$ and $\mathbf{E_2}$ are co-linear with the double-dashed system of Fig. 6.

Eq.'s (6) and (7) are both rotated into the materially embedded reference frame used by the FE code (triple dash system in Fig. 6), via a user subroutine. The rotated equations are added to find the final combined stress in this system. An attractive feature of this non-orthogonal model is that, given the shear angle, θ, the two shear parameters G_1 and G_2 can be related analytically to the shear force versus shear angle response of textile composites through Eq.'s (8) and (9).

$$G_1 = \frac{1}{lh}\left\{\frac{dF_s}{d\theta}\sqrt{g^{11}} + F_s\sqrt{g^{11}\left(g^{11}-1\right)}\right\} \tag{8}$$

$$G_2 = \left(\frac{F_s}{lh}\right)\sqrt{g^{11}} \tag{9}$$

where F_s is the shear force, which can be approximated using a polynomial function of θ and $dF_s/d\theta$ is the gradient of the shear force versus shear angle curve which is also a function of θ.

4. IMPLEMENTATION OF ENERGY MODEL

The energy model described in Section 2 requires the following material properties as input in order to generate shear force versus shear angle predictions: fibre volume fraction, matrix rheology, weave architecture and fibre diameter. For thermoplastic textile composites the matrix rheology is a function of shear strain rate and temperature. By specifying the temperature, the energy model allows prediction of a shear force surface in shear angle – angular velocity space. Using the input data for a twill weave glass/polypropylene thermoplastic textile composite with a fibre volume fraction of 0.35 for which the matrix rheology has been characterised using an RMS 800 Rheometer, predictions have been made and found to give excellent comparison with experimental results [4, 5]. An example of the predicted shear force surface for this thermoplastic composite is shown in Fig 8.

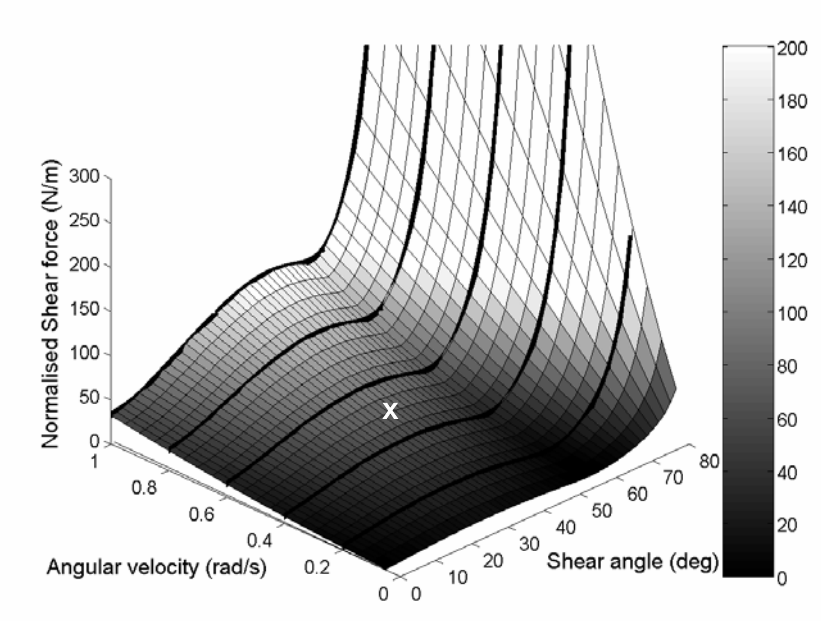

Fig 8. Shear force – shear angle – angular velocity prediction for twill weave glass/polypropylene thermoplastic textile composite at 190°C. Grey scale indicates the shear force magnitude of the surface (legend on right). The five thick black lines are 11th order polynomial fits to the surface at specific angular velocities: 0.2, 0.4, 0.6, 0.8 and 1 rads^{-1}. The white cross corresponds to the shear angle and angular velocity associated with a specific element (see text).

In order to incorporate these predictions in the FE code and consequently introduce rate dependency in the simulation, polynomial fits are made to the surface at specific angular velocities. In Fig. 8, five different fits to the energy model predictions are indicated by the thick black lines superimposed on the shear force surface. The polynomial coefficients of these fits and corresponding angular velocities are stored in a vector matrix. This is the output of the energy model and is stored in a text file in a specified location in the computer memory.

At the start of the FE simulation (so far the implementation of the energy model has been performed only in Abaqus Explicit^{TM}) the output of the energy model is read in matrix format into a specified variable. Care is taken to ensure that the code reads the data only one time, as repeated reading at each time step could slow the simulation significantly. During the FE simulation the angular velocities of the individual finite elements are calculated in the user subroutine (a Fortran program containing the FE implementation of the non-orthogonal constitutive model). This is done for each element and at each time step of the simulation. The code uses the angular velocity of the element to determine which polynomial curve approximation of the shear force – shear angle predictions will be used to calculate G_1 and G_2 using Eq.'s (8) and (9). This process is illustrated in Fig. 8. The white cross on the shear force surface indicates the shear angle ($\approx 35^o$) and angular velocity ($\approx 0.5\,\text{rads}^{-1}$) of a given element at a given time. In determining the shear parameters of this element, G_1 and G_2, the code assigns to the element the coefficients of the polynomial curve fitted at an angular velocity higher but contiguous with the angular velocity of the element. In this case the element would be assigned the polynomial coefficients of the 0.6 rads^{-1} curve.

5. PRELIMINARY FINITE ELEMENT RESULTS

A simulation of a hemisphere press forming process (see Fig. 9) has been conducted. Fig. 10 consists of fifteen images predicted from a single FE simulation. Rows correspond to different instances in time (0.002, 0.012, 0.024, 0.036, 0.06 sec, time increasing downwards) and columns correspond to three state variables: magnitude of shear angle, magnitude of angular velocity during time step and a polynomial curve indicator value (viewed from left to right). The indicator value is assigned to each element at the same time as the polynomial coefficients and serves to indicate which polynomial curve has been fitted to a given element. In this simulation the indicator value ranges from one to five corresponding to the five polynomial curve fits shown in Fig. 8. The indicator value has been used to check the correct functioning of the code. 6867 triangular membrane elements were used in creating the FE mesh of the blank.

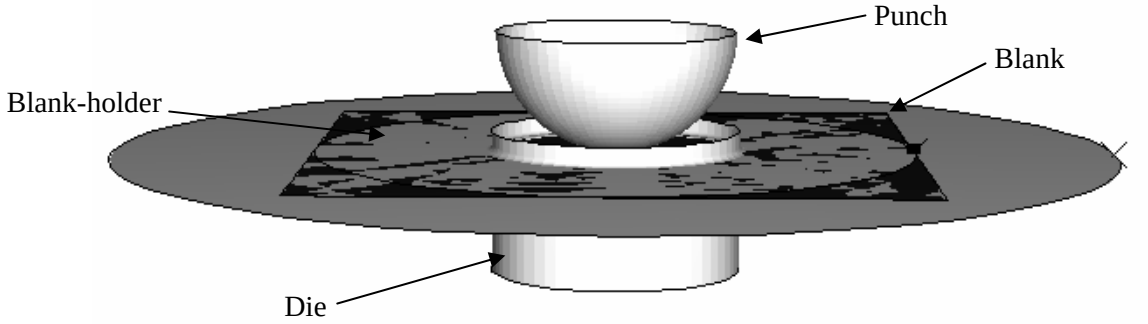

Fig 9. Hemisphere forming simulation set-up.

Note that the total punch travel is 6 cm over a total time of 0.06 seconds. Thus, the punch speed is 1 ms^{-1}, a speed that in practice would produce angular velocities far higher than 1 rads^{-1}. In order to induce angular velocities corresponding to the predictions of the energy model (see Fig. 8) a

velocity scale factor has been introduced in the user subroutine. The modified angular velocity is used purely as a reference in choosing the correct polynomial coefficients and has no bearing on the FE calculations.

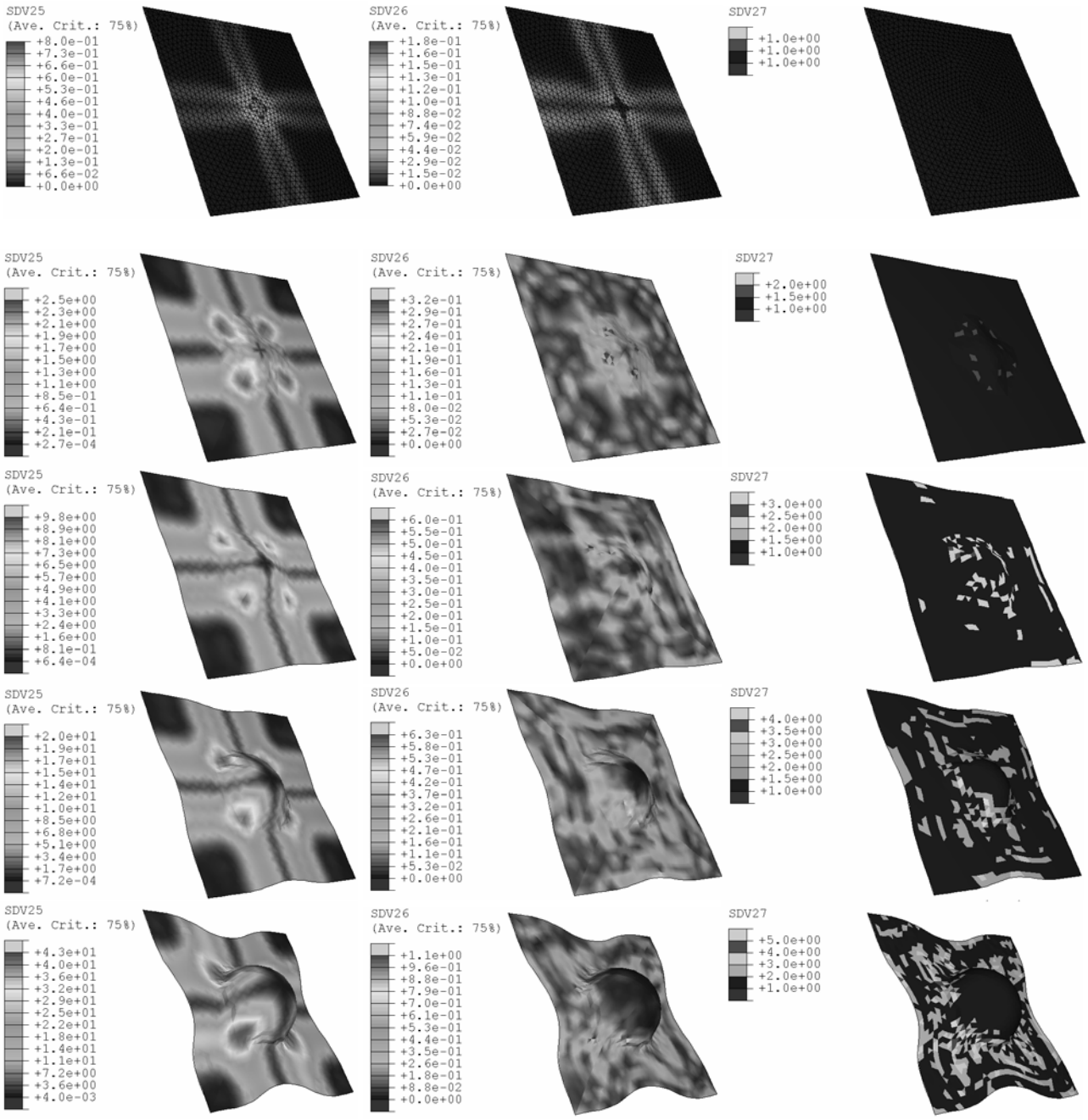

Fig 10. FE simulation of hemisphere forming. The rows correspond to increasing time, (0.002, 0.012, 0.024, 0.036, 0.06 sec, time increasing downwards) and columns correspond, from left to right, to: magnitude of shear angle, magnitude of angular velocity and a polynomial curve indicator value. The FE mesh of the blank is shown in the first time increment, 6867 triangular membrane elements were used in total.

Inspection of Fig. 10 show that different polynomial curves are indeed assigned to represent the shear behaviour of each element as the angular shear rate of the elements increase during the course of the simulation. Thus, the user subroutine successfully combines the two models and simulates rate dependent behaviour. By increasing the number of polynomial fits to the energy model predictions, the accuracy in modelling the rate behaviour would improve.

Images of the angular velocity (column 2 in Fig. 10) show that in any given time step this variable changes considerably across the sheet in an apparently random and patchy manner. This is thought to be due to the nature of the explicit FE code solver. Each individual element may contain an error in any given time-step (12,000 in this simulation). However, the time averaged value of the angular velocity is shown to be correct through the reasonable prediction of the shear angle (column 1 in Fig. 10), i.e. the shear angle in each element is effectively the angular velocity of each element integrated over time.

6. CONCLUSIONS

A constituent-based micro-mechanical energy model has been used to predict the shear parameters of a constitutive model featuring two non-orthogonal directions of fibre reinforcement. Given the matrix rheology, fibre volume fraction and fabric architecture, the combined implementation of the two models can be used to predict rate-dependent and temperature forming behaviour of any viscous textile composite, without the need for an extensive set of pre-simulation textile composite characterisation experiments. Preliminary FE simulations of hemisphere forming have demonstrated the successful combined implementation of the two models in a commercial explicit FE code.

ACKNOWLEDGEMENTS

We would like to thank the following organisations for their support: Univerisity of Cambridge, DSTL Farnborough, ESI Software, Ford Motor Company Ltd., Granta Design Ltd, Hexcel, MSC Software Ltd, Polynorm Plastics (UK) Ltd, Vetrotex International SA

References

[1] Yu, W.R., Pourboghrat, F., Chung, K. Zampaloni, M. and Kang, T.J., "Non-orthogonal constitutive equation for woven fabric reinforced thermoplastic composites." *Comp Part A-App S*, 33, (2002), 1095-1105

[2] Yu W.R., Harrison P. and Long A.C. "Finite Element Forming Simulation for Non-crimp Fabrics using a Non-Orthogonal Constitutive Equation" *(submitted to Comp Part A-App S, December 2003)*

[3] Harrison, P., Clifford, M.J., Long, A.C. and Rudd, C.D. "Constitutive modelling of impregnated continuous fibre reinforced composites: a micro-mechanical approach." *Plast Rubber Compos*, 2/31, (2002), 76-86

[4] Harrison, P., Clifford, M.J., Long, A.C. and Rudd, C.D. "A constitutive model for pre-impregnated viscous textile composites", *(accepted to Comp Part A-App S, September 2003)*

[5] Harrison, P., Clifford, M.J., Long, A.C. "Shear characterisation of woven textile composites: a comparison between picture frame and bias extension experiments", *(accepted to Compos Sci Technol, October 2003)*

[6] Rogers, T.G., "Rheological characterisation of anisotropic materials." *Composites*, 20/1, (1989), 21-27

[7] Christensen, R.M. "Effective viscous flow properties for fibre suspensions under concentrated conditions." *J Rheol*, 37/1, (1993), 103-121

[8] Coffin, D.W., Pipes, R.B. and Simacek, P., "First-order approximations for the effective shearing viscosities of continuous-fiber suspensions." *J Compos Mater*, 29/9, (1995), 1196-1180

[9] Shuler, S.F. and Advani, S.G. "Transverse squeeze flow of concentrated aligned fibers in viscous fluids." *J Non-Newton Fluid*, 65, (1996), 47-74

[10] Martin, T.A., Bhattacharyya, D. and Collins, I.F. "Bending of fibre-reinforced thermoplastic sheets." *Compos Manuf*, 6, (1995), 177-187

[11] McGuiness, G.B. and O'Bradaigh, C.M. "Characterisation of thermoplastic composite melts in rhombus-shear: the picture frame experiment." *Comp Part A-App S*, 29A, (1998), 115-132

[12] Spencer, A.J.M., "Theory of fabric-reinforced viscous fluids." *Comp Part A-App S A*, 31, (2000), 1311-1321

[13] McGuiness, G.B. and O'Bradaigh, C.M. "Development of rheological models for forming flows and picture frame testing of fabric reinforced thermoplastic sheets." *J Non-Newton Fluid*, 73, (1997), 1-28

[14] McGuiness, G.B., Canavan, R.A., Nestor, T.A. and O'Bradaigh, M.O. "A picture frame intra-ply sheet forming of composite materials." *Proc. ASME Materials Division, ASME*, (1995), 1107-1118